Supplemental Material: Hybrid $\mathbf{k}\cdot\mathbf{p}$-tight binding model for subbands and infrared intersubband optics in few-layer films of transition metal dichalcogenides: MoS_2, $MoSe_2$, WS_2, and WSe_2

David A. Ruiz-Tijerina,[1] Mark Danovich,[1] Celal Yelgel,[1] Viktor Zólyomi,[1] and Vladimir I. Fal'ko[1]

[1]*National Graphene Institute, University of Manchester, Booth St E, Manchester M13 9PL, UK*

(Dated: June 16, 2018)

I. DENSITY FUNCTIONAL THEORY BAND STRUCTURES FOR FEW-LAYER MoS_2, $MoSe_2$, WS_2 AND WSe_2

In Figs. S1 to S4 we show the band structures of 2H-stacked N-layer ($N = 1$ to 6) MoS_2, $MoSe_2$, WS_2 and WSe_2, obtained from density functional theory (DFT), which were used for the model parametrization. As discussed in Sec. II of the main text, our DFT calculations were performed using the Quantum Espresso [1] PWSCF *ab initio* package, choosing a plane-wave basis within the local density approximation (LDA), and using the Perdew-Zunger exchange correlation scheme [2], with fully-relativistic norm-conserving pseudo-potentials. The interlayer separations of the four transition-metal dichalcogenides (TMDs) were taken to be the experimental values 6.149 Å [3], 6.463 Å [4], 6.173 Å [5], and 6.477 Å [6], with LDA-optimized in-plane lattice constants 3.157 Å, 3.288 Å, 3.161 Å, and 3.291 Å, for MoS_2, $MoSe_2$, WS_2, and WSe_2, respectively. Further details of the DFT calculations can be found in Sec. II of the main text.

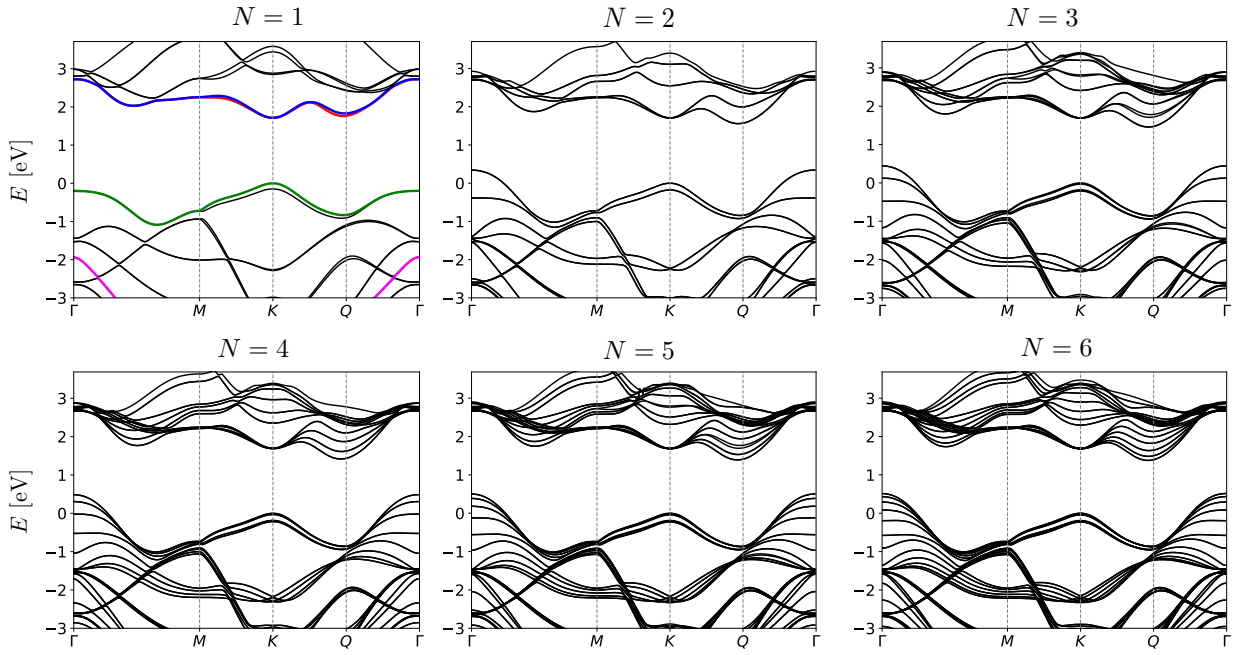

FIG. S1. DFT-calculated band structure of N-layer 2H-MoS_2, for $N = 1$ to 6. In the monolayer case, we highlight the conduction band (blue for spin down, red for spin up), valence band (green), and lower valence band w (magenta). Few-layer MoS_2 band structures have been presented in Refs. 7–11.

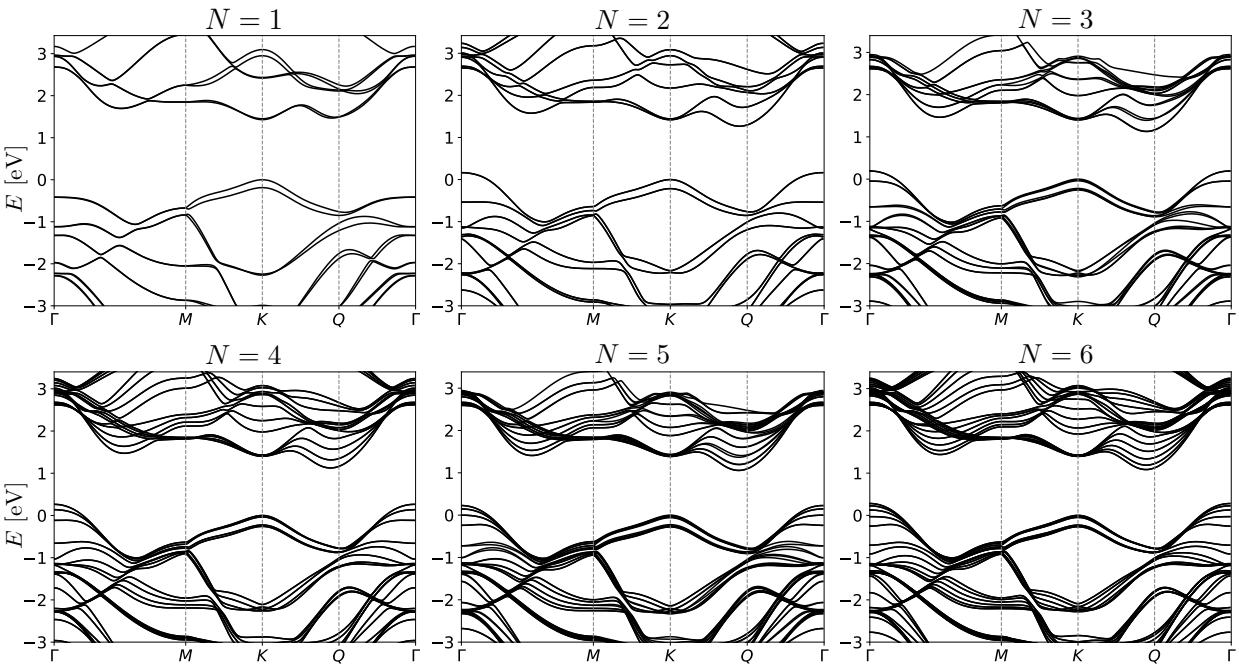

FIG. S2. DFT-calculated band structure of N-layer 2H-$MoSe_2$, for $N = 1$ to 6. Few-layer $MoSe_2$ band structures have been presented in Refs. 8, 10, 12, and 13.

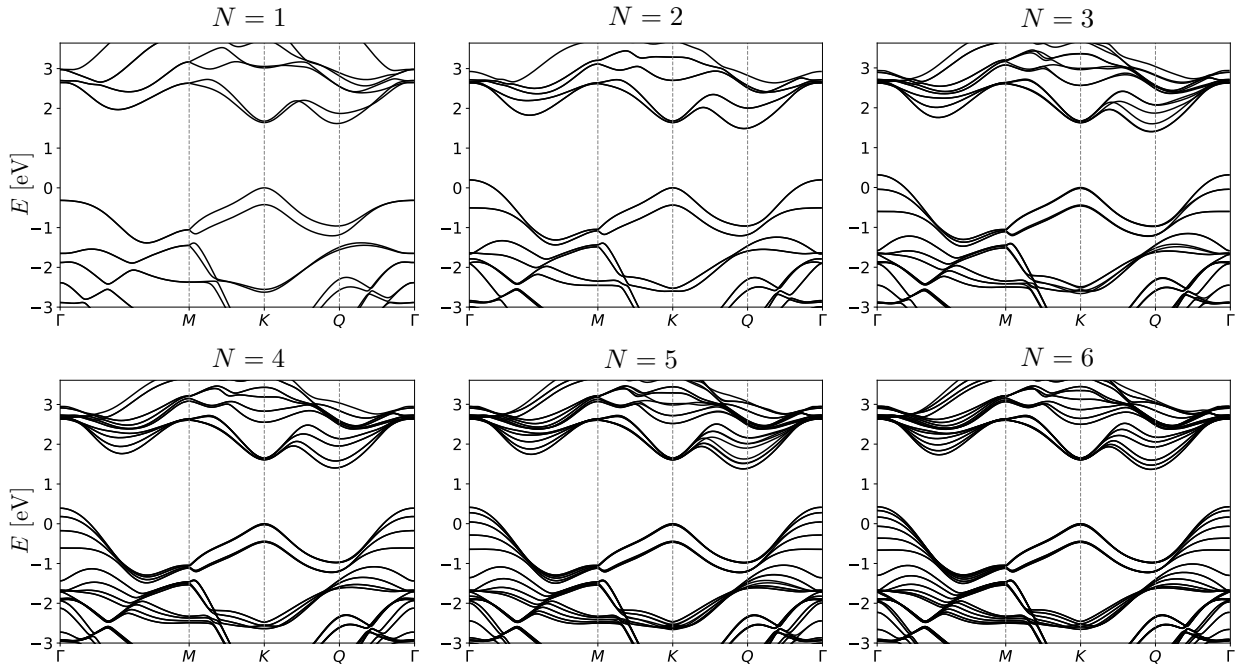

FIG. S3. DFT-calculated band structure of N-layer 2H-WS_2, for $N = 1$ to 6. Few-layer WS_2 band structures have been presented in Refs. 8 and 10.

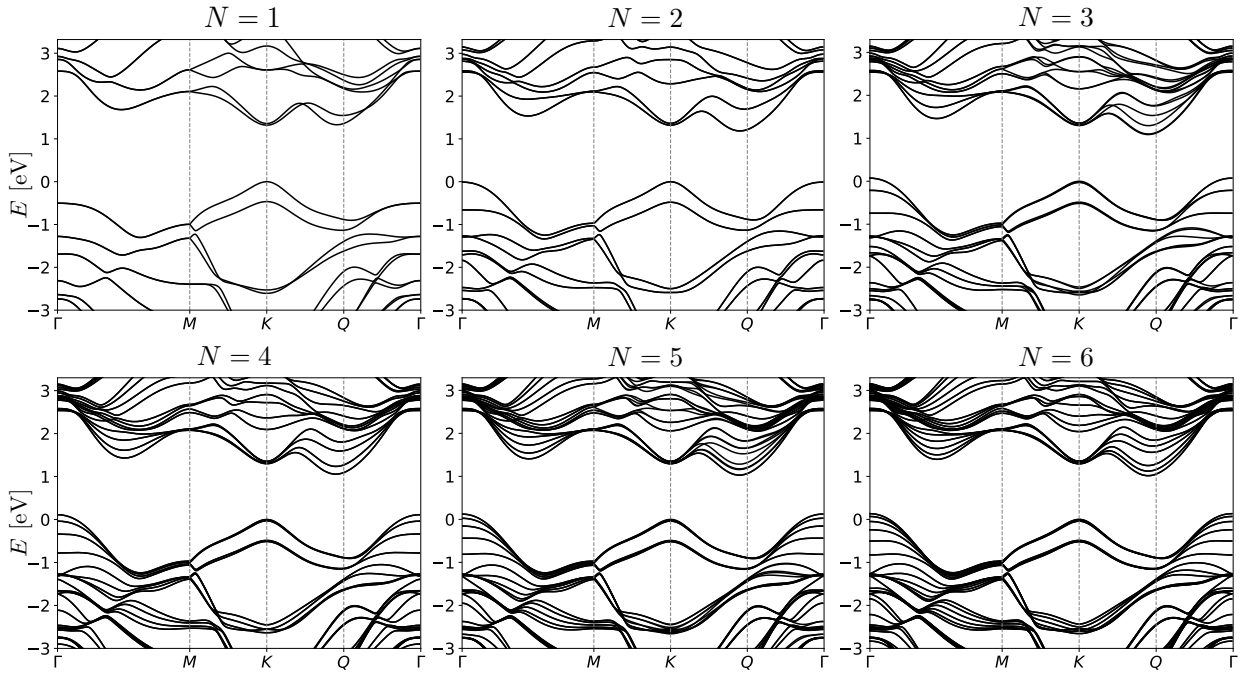

FIG. S4. DFT-calculated band structure of N-layer 2H-WSe_2, for $N = 1$ to 6. Few-layer WSe_2 band structures have been presented in Refs. 8, 10, and 13.

II. SAMPLE FITTINGS FOR THE HkpTB MODELS TO DFT SUBBAND STRUCTURES FOR FEW-LAYER MoS_2, $MoSe_2$, WS_2 AND WSe_2

Figs. S5 and S6 show sample fittings of our hybrid $\mathbf{k}\cdot\mathbf{p}$-tight-binding models (HkpTB) for the valence subbands near the Γ-point, and the conduction subbands near the Q-point, respectively, to the DFT band structures of all four TMDs shown in Sec. I. These, together with the fittings to the DFT bulk band structures shown in main text Figs. 3 and 9, were used to evaluate the model parameters presented in Tables I, II, IV and V of the main text.

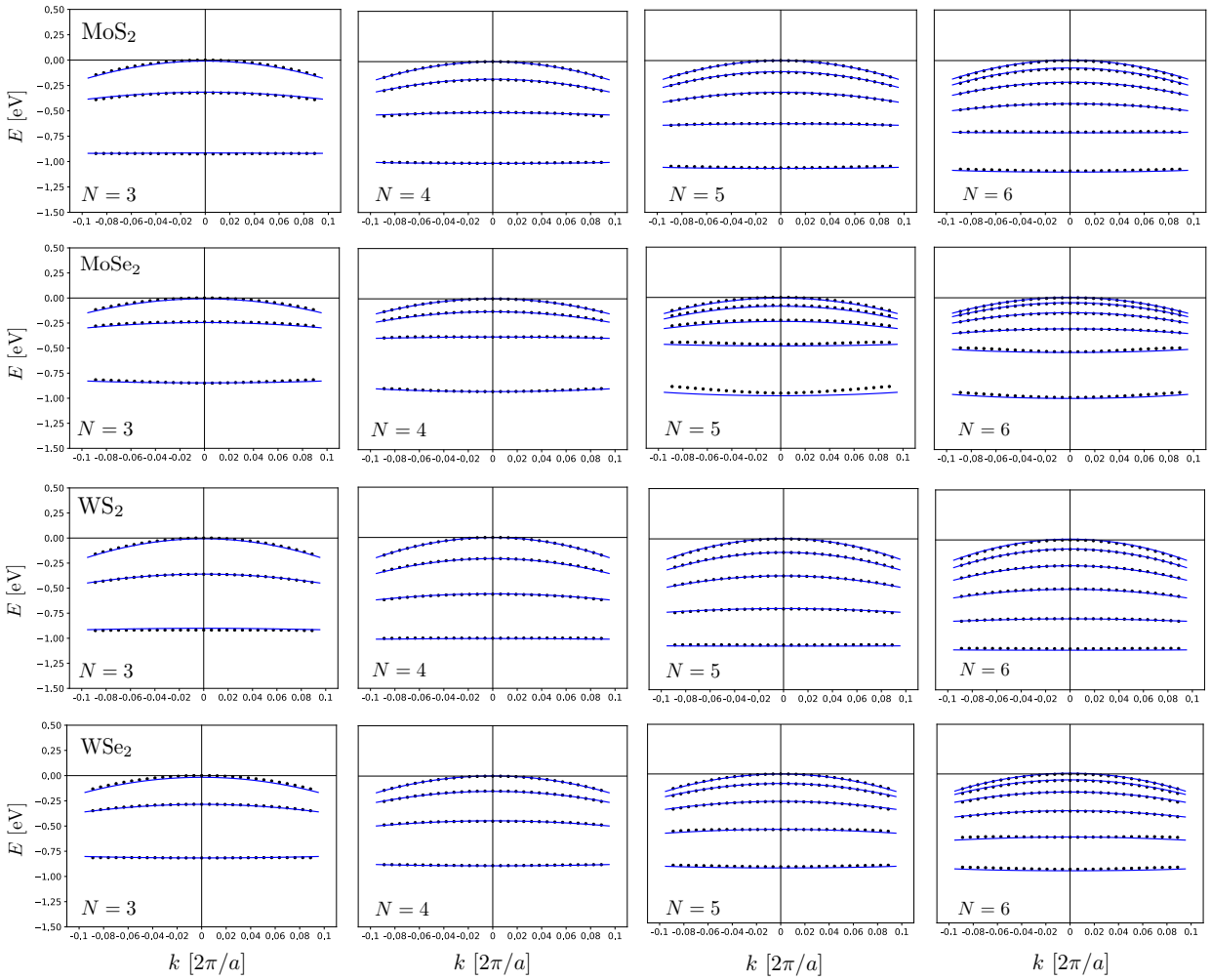

FIG. S5. Comparison between our HkpTB model (solid lines) and DFT results (points) for the valence subbands of 2H-stacked N-layer films ($N = 3$ to 6) of all four TMDs, near the Γ-point.

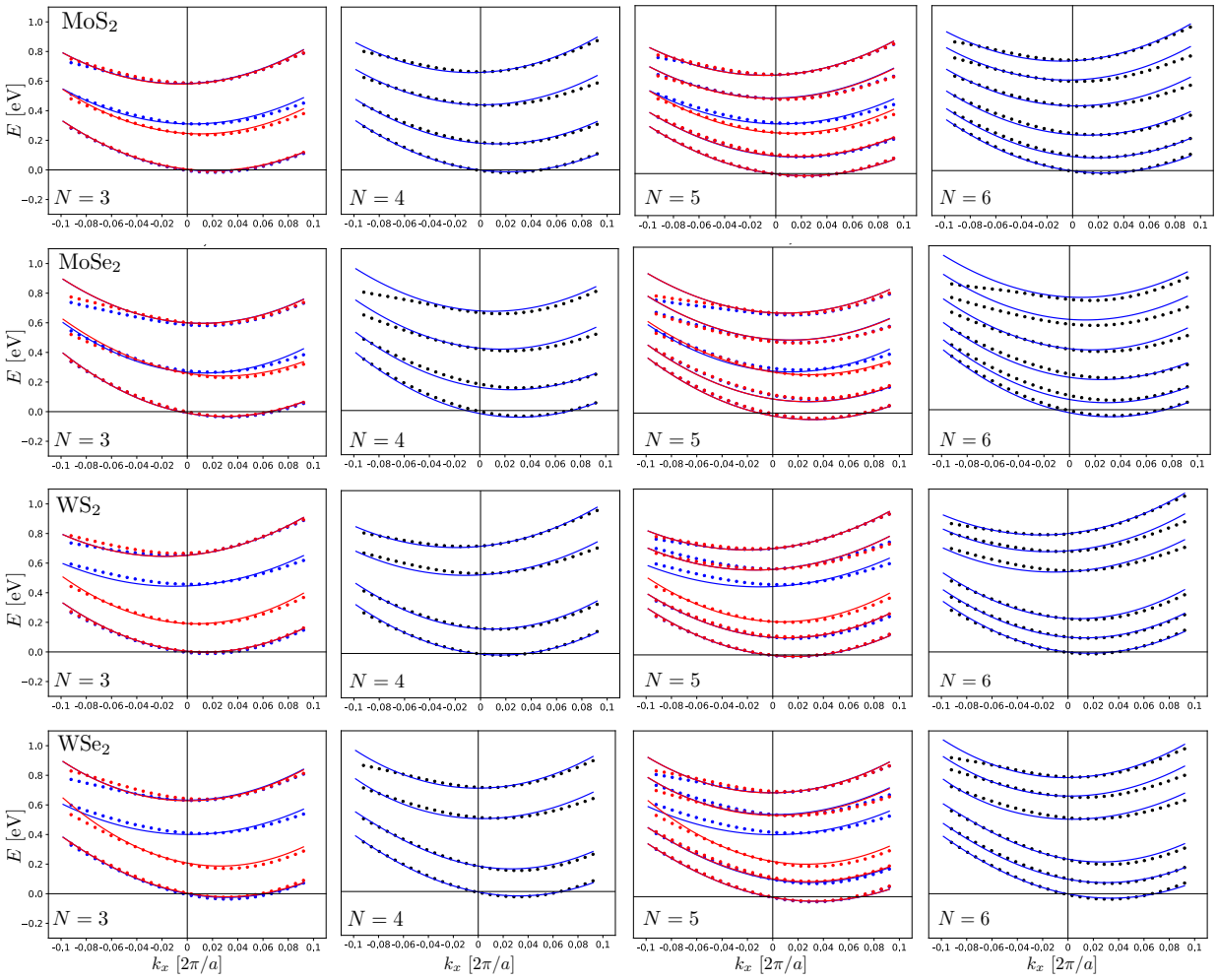

FIG. S6. Comparison between our HkpTB model (solid lines) and DFT results (points) for the conduction subbands of N-layer films ($N = 3$ to 6) of all four TMDs, near the Q-point ($k_x = 0$). For odd number of layers, the colors indicate the subband spin projection, with blue (red) corresponding to spin-down (spin-up); whereas for even number of layers, both spin projections are degenerate and shown in black points.

[1] P. Giannozzi, S. Baroni, N. Bonini, M. Calandra, R. Car, C. Cavazzoni, D. Ceresoli, G. L. Chiarotti, M. Cococcioni, I. Dabo, A. D. Corso, S. de Gironcoli, S. Fabris, G. Fratesi, R. Gebauer, U. Gerstmann, C. Gougoussis, A. Kokalj, M. Lazzeri, L. Martin-Samos, N. Marzari, F. Mauri, R. Mazzarello, S. Paolini, A. Pasquarello, L. Paulatto, C. Sbraccia,

S. Scandolo, G. Sclauzero, A. P. Seitsonen, A. Smogunov, P. Umari, and R. M. Wentzcovitch, Journal of Physics: Condensed Matter **21**, 395502 (2009).

[2] J. P. Perdew and A. Zunger, Phys. Rev. B **23**, 5048 (1981).

[3] T. Böker, R. Severin, A. Müller, C. Janowitz, R. Manzke, D. Voß, P. Krüger, A. Mazur, and J. Pollmann, Phys. Rev. B **64**, 235305 (2001).

[4] A. A. Al-Hilli and B. L. Evans, Journal of Crystal Growth **15**, 93 (1972).

[5] T. J. Wieting, Journal of Physics and Chemistry of Solids **31**, 2148 (1970).

[6] W. T. Hicks, Journal of The Electrochemical Society **111**, 1058 (1964), http://jes.ecsdl.org/content/111/9/1058.full.pdf+html.

[7] T. Cheiwchanchamnangij and W. R. L. Lambrecht, Phys. Rev. B **85**, 205302 (2012).

[8] L. Debbichi, O. Eriksson, and S. Lebègue, Phys. Rev. B **89**, 205311 (2014).

[9] J. E. Padilha, H. Peelaers, A. Janotti, and C. G. Van de Walle, Phys. Rev. B **90**, 205420 (2014).

[10] T.-R. Chang, H. Lin, H.-T. Jeng, and A. Bansil, Scientific Reports **4**, 6270 EP (2014).

[11] S. Fang, R. Kuate Defo, S. N. Shirodkar, S. Lieu, G. A. Tritsaris, and E. Kaxiras, Phys. Rev. B **92**, 205108 (2015).

[12] A. J. Bradley, M. M. Ugeda, F. H. da Jornada, D. Y. Qiu, W. Ruan, Y. Zhang, S. Wickenburg, A. Riss, J. Lu, S.-K. Mo, Z. Hussain, Z.-X. Shen, S. G. Louie, and M. F. Crommie, Nano Letters **15**, 2594 (2015), pMID: 25775022, http://dx.doi.org/10.1021/acs.nanolett.5b00160.

[13] Y. Sun, D. Wang, and Z. Shuai, The Journal of Physical Chemistry C **120**, 21866 (2016), http://dx.doi.org/10.1021/acs.jpcc.6b08748.